The September 2017 SEP event in context with the current solar cycle: Mars Express ASPERA-3/IMA and MAVEN/SEP observations

Robin Ramstad[1,2], Mats Holmström[1], Yoshifumi Futaana[1], Christina O. Lee[3], Ali Rahmati[3], Patrick Dunn[3], Robert J. Lillis[3], and Davin Larson[3]

Robin Ramstad, robin.ramstad@irf.se

[1]Swedish Institute of Space Physics, Kiruna, Sweden.

[2]Laboratory for Atmospheric and Space Physics, University of Colorado, Boulder, CO, USA.

[3]Space Sciences Laboratory, University of California, Berkeley, CA, USA.

This article has been accepted for publication and undergone full peer review but has not been through the copyediting, typesetting, pagination and proofreading process, which may lead to differences between this version and the Version of Record. Please cite this article as doi: 10.1029/2018GL077842

We use MAVEN/SEP energetic particle data to estimate the ranges of particle energies that generate background noise in the ASPERA-3/IMA instrument on Mars Express. The particles that generate IMA background counts are estimated to be electrons with energies >1 MeV and protons >20 MeV. The September 2017 event at Mars resulted in the strongest flux of energetic particles measured by MAVEN/SEP. We correspondingly use the IMA background data to compare this event with the rest of the last solar cycle and back to 2004, finding the event to be the 4$^{\text{th}}$ strongest SEP event detected by Mars Express.

Keypoints:

- IMA background counts provide the longest available record of penetrating energetic particles at Mars, covering more than a solar cycle.
- Comparison with MAVEN/SEP shows IMA to be sensitive to >1 MeV electrons and >20 MeV protons, with good correlation ($\rho = 0.85$).
- Distribution of IMA data shows the September 2017 event to be the 4$^{\text{th}}$ strongest SEP event observed by Mars Express (2004–2018).

1. Introduction

Energetic particles, i.e. ions and electrons with energies above several 10s of keV and generally up to a few GeV, permeate the solar system. Extrasolar sources generate Galactic Cosmic Rays (GCRs) which constitute a near-constant energetic particle background. Far more variable are fluxes of particles produced near the Sun, i.e. Solar Energetic Particles (SEPs). The strongest SEP fluxes are produced by solar flares and first-order Fermi acceleration at the shock boundaries of fast Coronal Mass Ejections (CMEs) that propagate through and pile-up the slower solar wind in their paths. While the induced magnetospheres of non-magnetized planets like Mars efficiently screen the bulk of the planetary ionospheres from the energy carried by the solar wind [*Ramstad et al.*, 2017] SEPs penetrate the induced magnetic barrier and precipitate into the planetary atmospheres, driving heating, dissociation and ionization rates. The bursts of intense penetrating radiation poses operational hazards to equipment and potential future human presence at Mars.

A few instruments have been designed to measure energetic particle fluxes near Mars, however, no instrument has provided a long-term record of the SEP environment. The Solar Low Energy Detector (SLED) instrument on the short-lived 1989 Phobos-2 mission only delivered data for ∼2 months [*McKenna-Lawlor et al.*, 1993]. The Mars Radiation Environment Experiment (MARIE) is installed on the still operational Mars Odyssey (2001–) orbiter [*Zeitlin et al.*, 2004], however MARIE ceased to function in October 2003. Lately the SEP investigation on the Mars Atmosphere and Volatile Evolution (MAVEN) mission has provided detailed measurements of the near-Mars energetic particle environ-

ment [*Larson et al.*, 2015; *Lillis et al.*, 2016], however MAVEN has currently only been in operation at Mars for about 3.5 years.

The Mars Express (MEX) orbiter (2003–) carries the Analyzer of Space Plasmas and Energetic Atoms (ASPERA-3) particles package, which includes the Ion Mass Analyzer (IMA) and Electron Spectrometer (ELS) instruments [*Barabash et al.*, 2006]. The top-hat electrostatic energy analyzers (ESAs) of IMA and ELS are only designed to measure ion and electron distributions up to 36 keV and 20 keV, respectively. However, sufficiently energetic particles can penetrate the walls and internal structure of the instruments and register as background counts on the microchannel plates (MCPs) [*Futaana et al.*, 2008]. The simultaneous presence of MEX and MAVEN at Mars since late 2014 presents an opportunity to estimate the IMA background energy sensitivity range and thus provide a long-term record of the SEP environment from 2004 to the present.

The Electron Reflectometer (ER) instrument on the Mars Global Surveyor (MGS, 1996–2006) orbiter also recorded spurious counts from penetrating energetic particles. *Delory et al.* [2012] estimated that MGS/ER was sensitive to >30 MeV particles and the dataset was used by *Lillis et al.* [2012] to study secondary electron emission during SEP events, demonstrating the scientific usefulness of such datasets. Indeed, a series of X-class flares and CMEs in September 2017 interrupted the late declining phase of the otherwise relatively calm 24$^{\text{th}}$ solar cycle and the effects were detected by several spacecraft at Mars (see the overview paper by *Lee et al.* [2018]). On September 10, on the onset of the arrival of a fast CME (4 protons/cm^3, 710 km/s, 3×10^5 K) MAVEN/SEP registered the strongest fluxes of energetic particles at Mars since the start of the mission. As can be seen in

Figure 1, the IMA background counts increased with a similar trend to the most energetic particles measured by MAVEN/SEP. The ASPERA-3/IMA background data allows us to quantify how extreme the September 2017 event was in comparison to the rest of solar cycle #24, and earlier, at Mars.

2. Method

The IMA ion-optics assembly consists of an electrostatic deflection system, sweeping elevation entrance angles for a top-hat ESA with an energy table covering 1 eV to 15 keV for most of the mission (since 2009). A post-acceleration ion lens energizes ions exiting the ESA by a set energy, 2433 eV for most orbits. A toroidal magnetic field subsequently separates the nearly monoenergetic ion beam by the gyroradii, i.e. mass-per-charge, of the constituent species, which is registered by impact location on an MCP segmented in 16 azimuthal and 32 radial anodes (mass-rings). The 96-step logarithmic energy table is covered every 12 s and the full energy-elevation table every 192 s. At high energies, above a few keV, the outermost mass-rings would correspond to ions with mass-per-charge below 1 amu/q. Counts registered by carefully chosen mass-rings can thus be assumed to be free of the intended signal of the instrument and rather represent the background noise. The methodology for isolating the average background count level is described by *Capalbo* [2010].

The SEP investigation on MAVEN constitutes 4 double-ended solid-state detector telescopes housed in two units (1 & 2) angled 90° relative each other and 45° relative the Sun in the nominal spacecraft attitude [*Larson et al.*, 2015]. Each telescope features an "open" aperture and a "foil" aperture, oriented opposite the other telescope in the same

unit. A permanent magnet imposes a magnetic field over the open aperture, deflecting electrons with energies <350 keV. Conversely, a sheet of Kapton foil covers the foil aperture, blocking ions with energies <250 keV. Three doped silicon detectors (F, T and O) in the telescope center allows determination of entrance direction and particle species by detection coincidence for electrons up to 600 keV and ions up to 11 MeV. Ions with energies $\gtrsim$11 MeV and electrons $\gtrsim$600 keV trigger all three detectors in a so-called FTO-event. Thus, MAVEN/SEP FTO-events provide information on fluxes of extremely high-energy SEPs, though without separation of particle species. While the native cadence of the instrument is 1 s, above 300 km the MAVEN/SEP data is accumulated onboard to 2, 4, or 8 s cadence before transmission to Earth.

To avoid SEP shadowing by the planet, we only use MAVEN and MEX data taken over 0.5 Martian radii in altitude [*Lillis et al.*, 2016], and only include MAVEN/SEP data recorded with the attenuator in the open state. The MAVEN/SEP data used here is exclusively from the SEP1B telescope since SEP1B has the open side nominally facing sunward roughly in the direction of the Parker spiral. Background IMA counts can be created by sources other than penetrating energetic particles. In certain narrow attitude ranges dense ionospheric plasma and solar UV can leak into the instrument and elevate the background level. To isolate the effects of energetic particles we only compare IMA and MAVEN/SEP measurements taken during SEP events. Five significant events, including the September 2017 event, were identified that are covered by both IMA and MAVEN/SEP, shown in Table 1.

A set of energy-dependent response values, R_i, corresponding to the MAVEN/SEP FTO energy bins, E_i, are optimized to find the energy response of IMA background. To find representative values for R_i we employ a genetic optimization algorithm designed to minimize the root of the sum of the squared residuals in log-space, i.e.

$$r = \sqrt{\sum \left(\log(C_{\mathrm{IMAbg}}) - \log \left(\sum_i R_i \times C_{\mathrm{SEP}}(E_i) \right) \right)^2}, \quad (1)$$

where the starting guess is 10^{-4} for all R_i. Each generation runs 1000 mutations randomly varying by up to 10 % relative the best guess of the previous generation. The first generation with an absolute relative change smaller than 10^{-6} is taken as the final estimate. In principle, with well-determined values for R_i, the average IMA background counts should be predictable from a given MAVEN/SEP FTO spectrum.

3. Results

A comparison of raw MAVEN/SEP FTO event counts and average IMA background counts is shown in Figure 2. Each FTO spectrum is compared to the average IMA background count using the genetic optimization algorithm to deduce the response values, R_i, shown in Figure 3.

From the shape of the response values it would appear that IMA is most sensitive to FTO bins 10–12. FTO events in these bins are caused by $\gtrsim$1 MeV electrons and have FWHM responses to protons in the following energy bands 10: 150–400 MeV, 11: 80–220 MeV, 12: 50–150 MeV. However, the typical energy distribution during SEP events implies that a disproportional amount of the counts are produced by protons with lower energies, such that FTO bin 12 represents protons down to 20 MeV. Conversely, IMA appears only weakly sensitive to particles generating FTO events in bins 13–14, which

are insensitive to electrons and are largely responding to protons $\lesssim$20 MeV. IMA is not sensitive at all to the ∼10–20 MeV protons registering as FTO events in bins 15–17. However, IMA is clearly sensitive to particles generating FTO events in bins 6–9, which are strongly dominated by >1 MeV electrons, though protons with energies from several 100 MeV up to 1 GeV would be sorted to these bins. Protons with energies >1 GeV would be sorted exclusively to bin 6. Bins 0–5 only register noise. It should be noted that these energy ranges are preliminary estimates and part of ongoing work.

The distribution of IMA background counts over the last 14 years and the September 2017 event are displayed in Figure 4, clearly showing that the peak energetic particle flux during the September 2017 event was extreme in the $\gtrsim$1 MeV electron/>20 MeV proton energy ranges IMA appears most sensitive to. Only a handful of SEP events observed by Mars Express over last solar cycle reached intensities higher than the September 2017 event, which peaked at 606 background counts. The highest average background count recorded by IMA in the selected data was 1471 counts on 2012-01-27 23:52:00, followed by 1056 counts on 2011-06-06 13:55:21 and 700 counts on 2005-04-28 02:37:48. All counts are collected over a 12 s full energy sweep of the ESA.

4. Discussion and Conclusions

The lack of systematic separation of protons and electrons in the MAVEN/SEP FTO-data precludes determining to which type of particle IMA is most sensitive. Nevertheless, IMA appears sensitive to energetic >20 MeV protons and $\gtrsim$1 MeV electrons as both are expected to generate the counts measured in FTO bins 10–12, electrons dominating in bins 6–9, and only protons registering in bins 13–14. A lower limit ∼20 MeV for penetrating

protons is consistent with the ∼30 MeV lower energy limit for energetic particles triggering background counts in the MGS/ER instrument found by [*Delory et al.*, 2012]. Limits near these values are expected as required to penetrate the typical aluminium housings of electrostatic plasma analyzers.

The varying attitude of MEX is not taken into account in this study and may introduce some bias in the background data due to SEP shadowing by the spacecraft. However, the wide angular spread of SEP distributions [*Lillis et al.*, 2016] implies that this effect is likely small. Indeed, the strong correlation between IMA background counts and expected IMA background counts from MAVEN/SEP FTO data ($\rho = 0.85$ in log/log-space, Figure 3) demonstrates that the IMA data can be reliably used to estimate fluxes of energetic particles. In future studies we intend to calibrate the IMA background to physical fluxes as measured by MAVEN/SEP and properly account for the varying attitude of Mars Express.

The distribution of IMA background counts since 2004 shows that the SEP flux during the September 2017 event was extreme in the energy range for which IMA is sensitive to penetrating particles. Note that IMA has not operated continuously for the duration of the mission and some gaps exist in the coverage over time, thus this distribution technically only represents the periods observed by IMA. As such, the peak flux during the September 2017 event was the 4^{th} strongest observed by Mars Express since the beginning of the mission in 2004.

Acknowledgments. The Swedish contribution to the ASPERA-3 experiment is supported by funding from the Swedish National Space Board (SNSB). ASPERA-3 data are

publicly available via the ESA Planetary Science Archive and processed IMA average background counts can be retrieved from http://rhea.umea.irf.se/∼peje/mex/hk/bkg/. MAVEN/SEP data are publicly available via the NASA Planetary Data System.

References

Barabash, S., et al. (2006) The Analyzer of Space Plasmas and Energetic Atoms (ASPERA-3) for the Mars Express mission, *Space. Sci Rev.* 126, 1–4, 113–164, doi:10.1007/s11214-006-9124-8.

Capalbo, F. J. (2010) Background Analysis for IMA Sensor on ASPERA Instrument, *IRF technical report* 054.

Delory, G. T., J. G. Luhmann, D. Brain, R. J. Lillis, D. L. Mitchell, R. A. Mewaldt, and T. V. Falkenberg (2012) Energetic particles detected by the Electron Reflectometer instrument on the Mars Global Surveyor, 1999-2006, *Space Weather* 10, S06003, doi:10.1029/2012SW000781.

Futaana, Y., et al. (2008) Mars Express and Venus Express multi-point observations of geoeffective solar flare events in December 2006, *Planet. Space. Sci* 56, 6, 873–880, doi:10.1016/j.pss.2007.10.014.

Larson, D. E., et al. (2015) The MAVEN Solar Energetic Particle Investigation, *Space. Sci Rev.* 195, 1–4, 153–172, doi:10.1007/s11214-015-0218-z.

Lee, C., et al. (2018) Observations and Impacts of the 10 September 2017 Solar Events at Mars: An Overview, *Geophys. Res. Lett.*, this issue.

Lillis, R. J., D. A. Brain, G. T. Delory, D. L. Mitchell, J. G. Luhmann, and R. P. Lin (2012) Evidence for superthermal secondary electrons produced by SEP ionization

in the Martian atmosphere, *J. Geophys. Res. Planets*, 117, E03004, 2818–2829, doi:10.1029/2011JE003932.

Lillis, R. J., C. O. Lee, D. Larson, J. G. Luhmann, J. S. Halekas, J. E. P. Connerney, and B. Jakosky (2016) Shadowing and anisotropy of solar energetic ions at Mars measured by MAVEN during the March 2015 solar storm, *J. Geophys. Res. Space Physics*, 121, 4, 2818–2829, doi:10.1002/2015JA022327.

McKenna-Lawlor, S. M. P., V. Alfonin, Ye. Yereshenko, E. Keppler, E. Kirsch, and K. Schwingenschuh (1993) First identification in energetic particles of characteristic plasma boundaries at Mars and an account of various energetic particle populations *Planet. Space Sci.* 41, 5, 373–380, doi:10.1016/0032-0633(93)90071-9.

Ramstad, R., S. Barabash, Y. Futaana, H. Nilsson, X. D. Wang, and M. Holmström (2015) The Martian atmospheric ion escape rate dependence on solar wind and solar EUV conditions: 1. Seven years of Mars Express observations *J. Geophys. Res. Space Physics* 120, doi:10.1002/2015JE004816.

Ramstad, R., S. Barabash, Y. Futaana, H. Nilsson, and M. Holmström (2017) Global Mars – Solar wind coupling and ion escape, *J. Geophys. Res. Space Physics* 122, doi:10.1002/2017JA024306.

Zeitlin, C., et al. (2004) Overview of the Martian radiation environment experiment, *Adv. Space Res.* 33, 12, 2204–2410, doi:10.1016/S0273-1177(03)00514-3.

Table 1. List of events and corresponding time intervals used to compare Mars Express ASPERA-3/IMA and MAVEN/SEP data.

No.	Start time	End time
#1	2015-03-25	2015-03-27
#2	2015-05-05	2015-05-07
#3	2015-10-28	2015-11-09
#4	2016-01-06	2016-01-09
#5	2017-09-10	2017-09-23

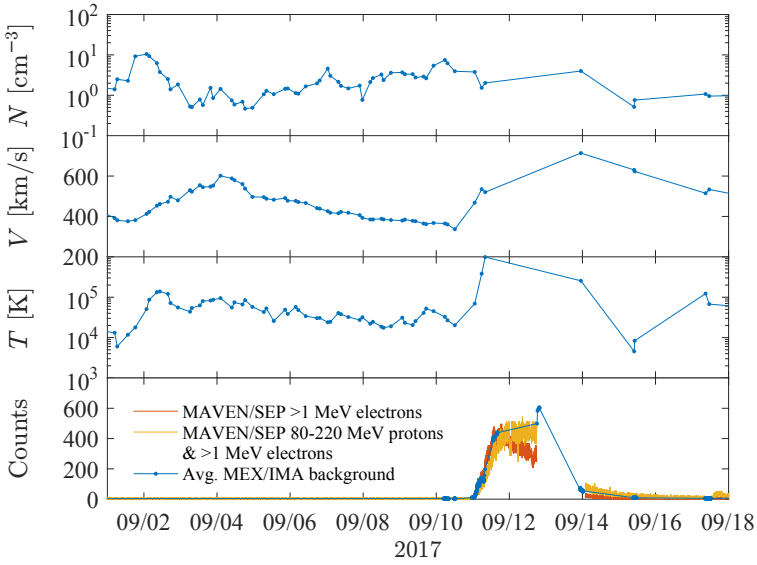

Figure 1. Solar wind moments (density, speed, temperature) measured by Mars Express ASPERA-3/IMA [*Ramstad et al.*, 2015]. The bottom panel shows energetic particles measured by the MAVEN/SEP investigation for different energies and types of particles, as well as average IMA background counts. The time-period is leading up to and including the September 2017 event. Note that the large intervals between MEX measurements are mainly due to limited operational time of ASPERA-3 in response to power conservation efforts for MEX during the 2017 eclipse season. The gap in MAVEN/SEP data excludes a period when the instrument attenuator was active.

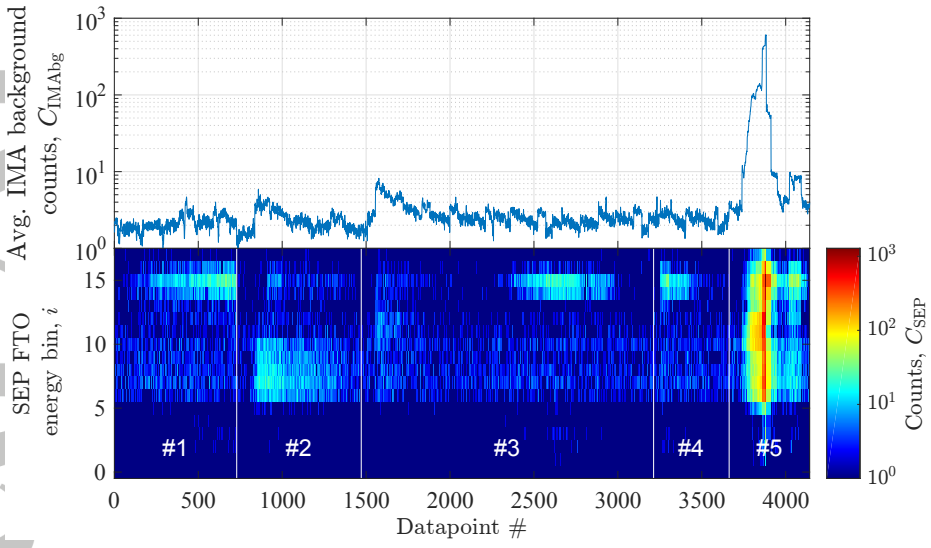

Figure 2. Average IMA background counts and raw MAVEN/SEP spectra for the five SEP events identified and utilized in this study, see Table 1.

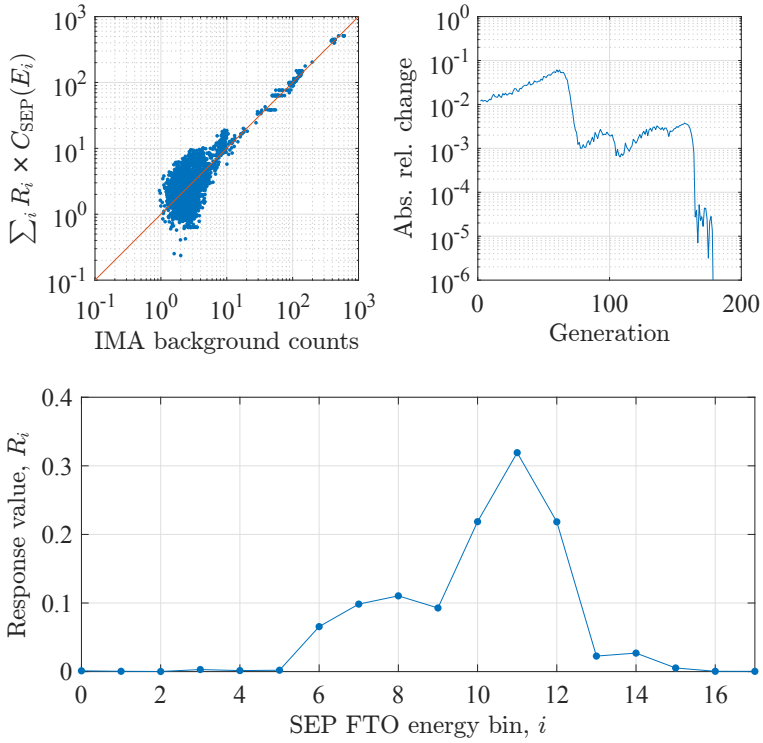

Figure 3. Result of the genetic optimization algorithm for obtaining the most representative energy response of the IMA background. Upper left panel: IMA background counts and reconstructed IMA background counts based on the final estimated response values. Upper right panel: Absolute relative change in the residual parameter, r, for each generation. Lower panel: Final estimation for the response values, R_i.

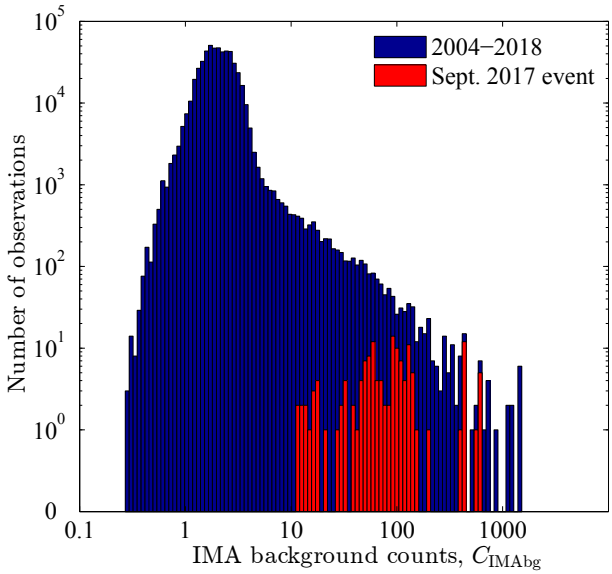

Figure 4. Distribution of average IMA background counts, each observed over the 12 s IMA energy sweeps, for the duration of the Mars Express mission (blue) and for the September 2017 event (red). The background counts higher than the peak counts from September 2017 were measured during three separate previous events in 2005, 2011 and 2012.